Modulation of Invasive Properties of CD133(+) Glioblastoma Stem Cells: A Role for MT1-MMP in Bioactive Lysophospholipid Signaling

Borhane Annabi,[1] Marie-Paule Lachambre,[2] Karine Plouffe,[2] Hervé Sartelet,[3] and Richard Béliveau[2]*

[1]*Laboratoire d'Oncologie Moléculaire, Département de Chimie, Université du Québec à Montréal, Montreal, Quebec, Canada*
[2]*Laboratoire de Médecine Moléculaire, Department of Neurosurgery, CHUM and UQAM, Montreal, Quebec, Canada*
[3]*Department of Pathology, Hôpital Sainte-Justine, Montreal, Quebec, Canada*

Future breakthroughs in cancer therapy must accompany targeted agents that will neutralize cancer stem cells response to circulating growth factors. Since the brain tissue microenvironmental niche is a prerequisite for expression of the stem cell marker CD133 antigen in brain tumors, we investigated the invasion mechanisms specific to CD133(+) U87 glioblastoma cells in response to lysophosphatidic acid (LPA) and sphingosine 1-phosphate (S1P), two circulating bioactive lysophospholipids and potent inducers of cancer. A CD133(+) U87 glioma cell population was isolated from parental U87 glioblastoma cells using magnetic cell sorting technology. The CD133(+)-enriched cell population grew as neurospheres and showed enhanced maximal response to both LPA (~5.0-fold) and S1P (~2.5-fold) at 1 µM when compared to parental U87 cells. The increased response to LPA in CD133(+) cells, reflected by increased levels of phosphorylated ERK, was found independent of the cooperative functions of the membrane-type-1 matrix metalloproteinase (MT1-MMP), while this cooperativity was essential to the S1P response. Quantitative RT-PCR was performed and we found higher gene expression levels of the S1P receptors S1P1 and S1P2, and of the LPA receptor LPA1 in CD133(+) cells than in their parental U87 cells. These increased levels reflected those observed from in vivo experimental U87 tumor implants. Our data suggest that the CD133(+) cell subpopulation evokes most of the lysophospholipid response within brain tumors through a combined regulation of S1P/LPA cell surface receptors signaling and by MT1-MMP. The emergence of lead compounds targeting the stem cell niche and S1P/LPA signaling in CD133(+) cancer cells is warranted. © 2009 Wiley-Liss, Inc.

Key words: cancer stem cells; glioblastoma; CD133; matrix metalloproteinases; endothelial differentiation gene

INTRODUCTION

Antiangiogenesis therapies are being increasingly adopted for treating glioblastomas, which are among the most angiogenic tumors [1,2]. Despite significant improvements, current therapies have yet to cure infiltrative gliomas which is possibly attributable to cancer stem cells (CSCs), a small subpopulation of cells within the brain tumor mass responsible for the initiation and maintenance of the tumor [3]. The idea that brain tumors arise from this specific subset of self-renewing, multipotent cells has gained great support [4–6] and CSC may therefore play a pivotal role in tumor initiation, growth, and recurrence. Accordingly, among the documented angiogenic factors, vascular endothelial growth factor (VEGF) promoted neurogenesis of neural stem cells [7]. Using VEGF-expressing CSC derived from human glioblastomas, it was revealed that VEGF induced the proliferation of vascular endothelial cells in the vascular-rich tumor environment, the so-called stem cell niche [8]. Whether alternate angiogenic growth factors, such as the bioactive lipids lysophosphatidic

acid (LPA) and sphingosine 1-phosphate (S1P), contribute to the etiology of cancer through regulation of CSC proliferation, survival, or migration is unknown.

The inherent signaling properties of S1P and LPA suggest, however, that both could regulate pathways involved in malignant transformation [9]. In fact, the receptors that receive their signals are all currently investigated as potential therapeutic targets in cancer [10]. S1P and LPA signal through a family of eight G-protein-coupled receptors, named

---

S1P(1-5) and LPA(1-3) [11]. S1P stimulates growth and invasiveness of glioma cells, and high expression levels of the enzyme that forms S1P, sphingosine kinase-1, correlate with short survival of glioma patients [12,13]. Recently, small populations of CSC in adult and pediatric brain tumors were identified [14,15]. These CSC, once isolated from tumor tissues, form neurospheres when cultured in vitro and possess the capacity for cell renewal. Based upon their high expression of the neural precursor cell surface marker CD133 (prominin-1), these CSC have been further hypothesized to bear properties such as resistance to apoptosis and resistance to both drugs and ionizing radiation [16,17]. Whether LPA- and S1P-mediated activities might contribute to any CD133(+) CSC response during brain tumor development is currently unknown.

Increased invasiveness in CD133(+) DAOY medulloblastoma cells was also demonstrated by us to involve the expression of a membrane-type-1 matrix metalloproteinase (MT1-MMP) [18]. MT1-MMP functions have been shown to be essential for cell migration and cooperated with S1P-mediated signaling in endothelial cells [19], mesenchymal stromal cells [20,21] and in U87 glioblastoma cells [22]. Interestingly, gene silencing of MT1-MMP in glioblastoma cells was found to abrogate S1P-mediated intracellular calcium mobilization, confirming a relationship between lysophospholipid metabolism/signaling and MMP-mediated extracellular matrix degradation [22]. Furthermore, MT1-MMP-increased expression and function in proMMP-2 activation were also observed in CD133(+) neurospheres isolated from pediatric brain tumor-derived DAOY medulloblastoma cells [18]. Future breakthroughs in cancer therapy must accompany targeted agents that will neutralize CSC response to circulating growth factors. In the current study, we examined the mechanism of S1P and LPA stimulation of parental and CD133-enriched glioma cell invasion as well as the different gene expression profiles of their cell surface receptors. We further examined the impact of MT1-MMP on CD133(+) glioma cell migration in response to S1P and LPA.

MATERIALS AND METHODS

Materials

Sodium dodecylsulfate (SDS) and bovine serum albumin (BSA) were purchased from Sigma (Oakville, Canada). Cell culture media was obtained from Life Technologies (Burlington, Canada). The rabbit polyclonal antibody against CD133 was generated against a synthetic peptide (KDHVYGIHNPVMTSPSQH) corresponding to the c-terminal amino acids 848–865 (ab16518, Abcam, Cambridge, MA). Electrophoresis reagents were purchased from Bio-Rad (Mississauga, Canada). Micro bicinchoninic acid protein assay reagents were from Pierce (Rockford, IL). All other reagents were from Sigma–Aldrich (Oakville, Canada).

Cell Culture and MT1-MMP Gene Silencing Method

The U87 glioblastoma cell line was purchased from American Type Culture Collection (Manassas, VA) and cultured in Eagle's Minimum essential medium (MEM) containing 10% (v/v) fetal bovine serum (FBS) (HyClone Laboratories, Logan, UT) and 2 mM glutamine, at 37°C under a humidified atmosphere containing 5% CO_2. RNA interference experiments were performed using Lipofectamine 2000 (Invitrogen, Burlington, Canada). A small interfering RNA against MT1-MMP (siMT1-MMP) and mismatch siRNA were synthesized by EZBiolab, Inc. (Westfield, IN) and annealed to form duplexes. The sequence of the siMT1-MMP used in this study is as follows: 5'-CCAGAAGCUGAAGGUAGAAdTdT-3' (sense) and 5'-UUCUACCUUCAGCUUCUGGdTdT-3' (antisense) [23]. Transient transfections were performed with 20 nM siMT1-MMP and the occurrence of MT1-MMP specific gene knockdown was evaluated by semi-quantitative Reverse Transcriptasion-Polymerase Chain Reaction (RT-PCR) or validated by assessing MT1-MMP-mediated proMMP-2 activation in the presence of Concanavalin-A (ConA) [24]. The decrease in MT1-MMP expression, as assessed by RT-PCR, ranged routinely from 75% to 90% (not shown).

Magnetic Cell Sorting and Flow Cytometry

Confluent U87 glioma parental cells were harvested with cell dissociation buffer (Hank's based; Invitrogen), centrifuged at 800g for 5 min and resuspended in 1× PBS with 0.5% BSA and 2 mM EDTA. Magnetic labeling with 100 μL AC133 (CD133/1) Microbeads per 10^8 cells was performed for 30 min at 4°C using the Miltenyi Biotec CD133 Direct Cell Isolation kit. Fifty microliters of 293C3 (CD133–2)-phycoerythrin (fluorochrome-conjugated mouse monoclonal IgG2b; Miltenyi Biotec, Auburn, CA) was added for an additional 10 min at 4°C to evaluate the efficiency of magnetic separation by flow cytometry. Magnetic separation was carried out using LS columns and a MACS separator (Miltenyi Biotec) under a biological hood. CD133(+) fractions were eluted by removing the column from the magnetic field and using a sterile plunger. Aliquots of CD133(+)-sorted cells were evaluated for purity by flow cytometry with a FACSCalibur machine (BD Biosciences, Mississauga, Canada). CD133(+)-sorted cell populations were resuspended in SFM with growth hormones.

Intracranial Tumor Model

All animal experiments were evaluated and approved by the Institutional Committee for Good

Animal Practices (UQAM, Montreal, Canada). Intracerebral tumor implantation was performed as previously described with some modifications [18]. Anesthetized 5- to 10-wk-old Crl:CD-1®-nuBR female nude mice (Charles River, Canada) were placed in a stereotaxic frame; viable U-87 glioblastoma cells (5×10^4) in 5 μL of medium without serum were then implanted into the right corpus striatum at a depth of 3.5 mm at a point 2.5 mm lateral to the midline and 1.5 mm anterior to the bregma using a Hamilton syringe. The syringe was removed after 5 min and the wound was closed with sutures. Animals were killed between 28 and 30 d postimplantation.

Subcutaneous Xenograft Model

Tumor implantation was performed as described previously [18]. Briefly, U-87 glioblastoma cells were harvested by trypsinization using a trypsin/EDTA solution. Cells were washed three times with phosphate buffered saline that was free of both Ca^{2+} and Mg^{2+}, and centrifuged. The resulting pellet was resuspended in 1% methyl-cellulose in serum-free MEM at a concentration of 2.5×10^6 cells per 100 μL. Animals were anesthetized by O_2/isoflurane inhalation and tumors were established by subcutaneous injection of 100 μL from the cell suspension into the right flank of female Crl:CD-1®-nuBR nude mice. The tumor size was measured every 3 d using a digital caliper. Tumor size was calculated as follows: $\pi/6 \times$ length $\times$ width^2. Animals were sacrificed after 28–30 d postimplantation.

Histological Analysis, and Immunohistochemistry for Characterization of Cellular and Tumor Markers

Brains from mice were fixed in 10% buffered formalin and paraffin-embedded. For routine histological examination, 3 μm-thick sections were stained with hematoxylin-phloxin-saffron (HPS). Immunohistochemistry was performed on paraffin-embedded sections using Ultraview Universal DAB detection kit (Ventana Medical Systems, Tucson, AZ). Rabbit polyclonal antibodies against CD133 (1/100), CD31 (1/100; Santa Cruz Biotechnology, Santa Cruz, CA) and Ki67 (1/200, Neomarker, Fremont, CA) were applied. First, for antigen retrieval, deparaffinized and rehydrated sections were pretreated using a Cell conditioning 1 in BenchMark XT (Ventana Medical Systems). The slides were then incubated for 32 min with the diluted antibody, followed by application of Ultraview Universal DAB detection kit (Ventana Medical Systems). DAB was used as a chromogen and hematoxylin as a counterstain. A section of specific positive human control from fetal liver for CD133 [25], from normal mouse brain for CD31, and from normal human lymph node for Ki67 were used on the same slide. Normal mouse or rabbit IgG at the same concentration as the primary antibody served as negative controls.

Total RNA Isolation and Semi-Quantitative Reverse Transcriptasion-Polymerase Chain Reaction (RT-PCR) Analysis

Total RNA was extracted from cell monolayers using the TRIzol reagent (Life Technologies). One microgram of total RNA was used for first strand cDNA synthesis followed by specific gene product amplification with the One-Step RT-PCR Kit (Invitrogen). Primers for CD133 (Santa Cruz Biotechnology), S1P1-5, and LPA1-3 (QIAGEN, Valencia, CA) were all derived from human sequences. PCR conditions were optimized so that the gene products were examined at the exponential phase of their amplification and the products were resolved on 1.8% agarose gels containing 1 μg/mL ethidium bromide.

cDNA Synthesis and Real-Time Quantitative RT-PCR

Total RNA was extracted from fresh tumor tissue or cell cultures as described above. For cDNA synthesis, $\sim$1 μg total RNA was reverse-transcribed into cDNA using high capacity cDNA reverse transcription kit (Applied Biosystems, Foster City, CA). cDNA was stored at $-80°C$ for PCR. Gene expression was quantified by real-time quantitative PCR using iQ SYBR Green Supermix (BIO-RAD, Hercules, CA). DNA amplification was carried out using an Icycler iQ5 (BIO-RAD, Hercules, CA) and product detection was performed by measuring the binding of the fluorescent dye SYBR Green I to double-stranded DNA. All the primer sets were provided by QIAGEN. The relative quantities of target gene mRNA against an internal control, 18S ribosomal RNA, were measured by following a ΔC_T method. An amplification plot (fluorescence signal vs. cycle number) was drawn. The difference (ΔC_T) between the mean values in the triplicate samples of target gene and those of 18S ribosomal RNA were calculated by iQ5 Optical System Software version 2.0 (BIO-RAD, Hercules, CA) and the relative quantified value (RQV) was expressed as $2^{-\Delta C_T}$.

Immunoblotting Procedures

Proteins from control and treated cells were separated by SDS–polyacrylamide gel electrophoresis (PAGE). After electrophoresis, proteins were electrotransferred to polyvinylidene difluoride membranes which were then blocked for 1 h at room temperature with 5% nonfat dry milk in Tris-buffered saline (150 mM NaCl, 20 mM Tris-HCl, pH 7.5) containing 0.3% Tween-20 (TBST). Membranes were further washed in TBST and incubated with either CD133, extracellular signal-regulated kinase (ERK) or phosphorylated ERK primary antibodies (1/1,000 dilution) in TBST containing 3% BSA, followed by a 1 h incubation with horseradish peroxidase-conjugated anti-rabbit IgG (1/2,500 dilution) in TBST containing

5% nonfat dry milk. Immunoreactive material was visualized by enhanced chemiluminescence (Amersham Biosciences, Baie d'Urfée, Canada).

Gelatin zymography

Gelatin zymography was used to assess the induction of extracellular proMMP-2 to active MMP-2 in ConA-treated cells. Briefly, an aliquot (20 μL) of the culture medium was subjected to SDS–PAGE in a gel containing 0.1 mg/mL gelatin. The gels were then incubated in 2.5% Triton X-100 and rinsed in nanopure distilled H_2O. Gels were further incubated at 37°C for 20 h in 20 mM NaCl, 5 mM $CaCl_2$, 0.02% Brij-35, 50 mM Tris-HCl buffer, pH 7.6, then stained with 0.1% Coomassie Brilliant blue R-250 and distained in 10% acetic acid, 30% methanol in H_2O. Gelatinolytic activity was detected as unstained bands on a blue background.

Statistical Data Analysis

Data are representative of three or more independent experiments. Statistical significance was assessed using Student's unpaired t-test. Probability values of less than 0.05 were considered significant, and an asterisk (*) identifies such significance in each figure.

RESULTS

Evaluation of CD133 Protein Expression and S1P/LPA Receptors Gene Expression Profiles in Intra-Cranial Experimental Glioblastoma Tumors

In an attempt to assess the contribution of CD133(+) CSC to experimental brain tumor growth, monolayer cultures of U87 glioblastoma cells were trypsinized and cell suspensions were implanted either subcutaneously or by stereotaxis within the brain of nude mice and left to develop for several weeks as described in Materials and Methods Section. We found that U87 cells implanted subcutaneously or within the cerebral environment readily developed into tumors. Intracerebral growth of U87 tumors was routinely found to occur within the first 3–4 wk, and time-to-sacrifice was similar between intracerebral and subcutaneous implantations (~28–30 d) suggesting that tumor growth within each injected site affected the mice equivalently. Homogenates were then generated from the individual tumors and CD133 immunodetection was performed. We found that CD133 protein expression was only observed when U87 cells were implanted within the cerebral environment (Figure 1A). Histopathological analysis of intracerebrally implanted human U87 cells showed malignant proliferation composed of round and spindled cells. The mitoses were frequent and associated with necrosis (Figure 1B; HPS). A large majority of tumoral cells exhibited membranous expression of CD133
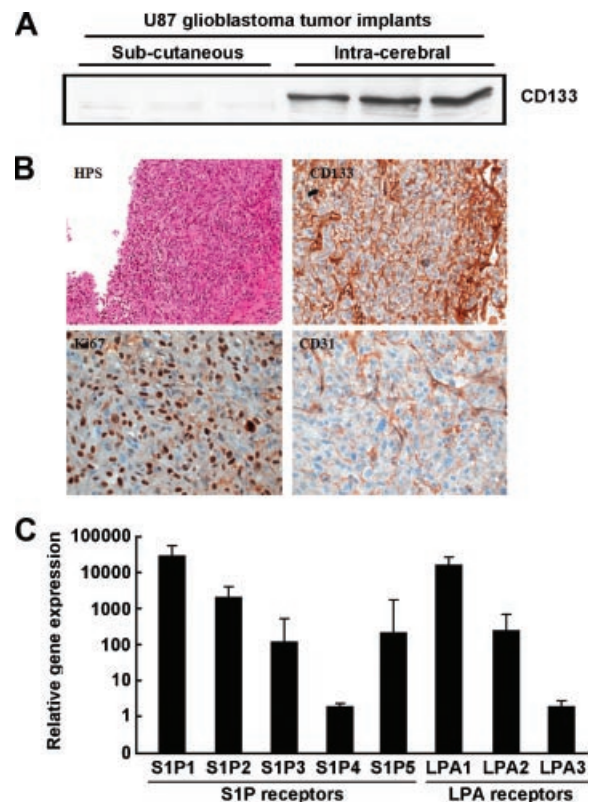

Figure 1. Evaluation of CD133 protein expression and S1P/LPA receptors gene expression profiles in intra-cranial experimental glioblastoma tumors. Cultured U87 monolayers were trypsinized and 10^6 cells injected subcutaneously (s.c.) or intra-cerebrally (i.c.) in nude mice. Tumors were left to develop as described in Materials and Methods Section. (A) Immunoblotting was used to assess CD133 protein expression in lysates (20 μg proteins) generated from subcutaneous and intracerebral U87 glioblastoma-implanted cells as described in Materials and Methods Section. (B) Histopathological analysis of paraffin sections (3 μm) of i.c. implanted human U87 glioblastoma cells was performed with hematoxylin-phloxin-saffron (HPS, original magnification 200×) staining and shows malignant proliferation, composed of a majority of small round cells with numerous mitoses. A large majority of tumoral cells exhibited a membranous expression of CD133 (>90%) (upper right panel, original magnification 400×). Ki67 staining was also performed in order to assess the cells in the G1, S, M, and G2-phases of the cell cycle, and it was highly expressed in tumoral cells (>40%) (lower left panel, original magnification 630×). Significant tumor-associated vascularization was observed, composed of capillaries detected by CD31 staining (platelet/endothelial cell-adhesion molecule-1) (lower right panel, original magnification 630×). (C) Total RNA was extracted from 3 i.c. tumor samples and gene expression profiles of the five S1P and three LPA receptors assessed by quantitative RT-PCR.

(>90%) (Figure 1B; CD133). Ki67 staining was also performed in order to assess the cells in the G1, S, M, and G2 phases of the cell cycle, and it was highly expressed in the tumor cells (>40%) (Figure 1B, Ki67). Significant tumor-associated vascularization was observed, composed of capillaries detected by CD31 staining (platelet/endothelial cell-adhesion molecule-1) (Figure 1B; CD31). Due to the lack of reliable commercial antibodies covering the complete five S1P and three LPA receptors panel, we chose to assess the gene expression profiles of S1P

receptors (S1P-1 to -5) and of LPA receptors (LPA-1 to -3) during in vivo experimental brain tumor growth. Total RNA was extracted from three different tumors and qRT-PCR was next performed to assess the expression of S1P and LPA receptors in the tumors. We found that S1P1, S1P2, as well as LPA1 were highly expressed in the U87 experimental brain tumors (Figure 1C). The different levels of expression for the various S1P/LPA receptors in CD133(+) cells as well as the extent of CD133(+) U87 glioma cells response to S1P or LPA that may contribute to the infiltrating phenotype of the tumor was next assessed.

Isolation of CD133(+) U87 Glioma Cells

In order to evaluate the potential contribution of the CD133(+) cell subpopulation, we used magnetic cell sorting (MACS) technology to isolate CD133(+) cells from the parental U87 glioma cell population [26]. We found that the CD133(+) U87 cell population represented ~0.15% of the total parental U87 glioma cells (Figure 2A, left panel). Sorting of the CD133(+) cells was then performed and we evaluated the cells as being ~27% CD133 positive (Figure 2A, right panel). The isolated subpopulation, with an enrichment of ~180-fold for CD133(+) U87 cells, was put into culture. Cell morphology of the parental and CD133(+) U87 glioma cells, was compared, and we observed that the CD133(+) cells formed spontaneous neurospheres, a characteristic of brain CSCs in agreement with previous reports [26] (Figure 2B). Total RNA was isolated from parental and CD133(+) glioma cells in order to assess gene expression levels

of CD133 (Figure 2C, white bars) and of β-actin (Figure 2C, black bars). We found that CD133 gene expression was increased by ~6-fold in the sorted CD133(+) U87 glioma cells, in agreement with the increased CD133 cell surface expression (Figure 2A, right panel).

Gene Expression Levels of the S1P/LPA Receptors in CD133(+) U87 Glioma Cells

We next assessed the contribution of CD133(+) U87 cells to the overall S1P/LPA receptors gene expression observed in the experimental U87 implanted glioma tumors. The initial relative gene expression levels of the S1P and LPA receptors in parental and in sorted CD133(+) U87 cells was assessed using RT-PCR. Semi-quantitative RT-PCR validation was first performed in order to show that one cDNA amplicon was associated with each of the five S1P (S1P-1 to -5) and three LPA (LPA1 to -3). All of the S1P and LPA receptors gene could be amplified as demonstrated by agarose gel electrophoresis (Figure 3A). Quantitative RT-PCR was next performed and we found that S1P1, S1P2, S1P4, LPA1, and LPA3 gene expression levels were significantly higher in CD133(+) U87 cells than in the parental U87 cells (Figure 3B). When compared to the in vivo setting as documented in the experimentally implanted intracranial tumor (Figure 1), good correlation is observed overall for most S1P and LPA receptors gene expression in cell cultures in vitro except for S1P4 and LPA3 which are found significantly increased in CD133(+) cells (Figure 3C). Whether any paracrine regulation occurs within
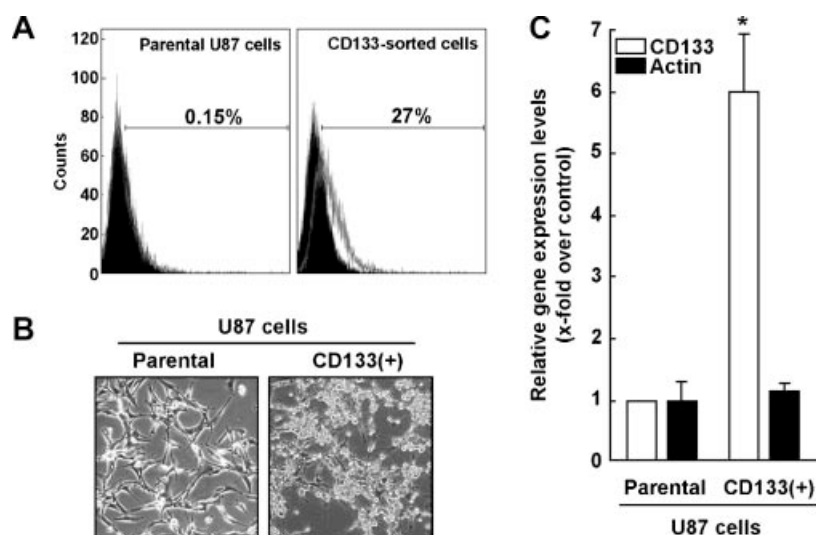

Figure 2. Isolation of CD133(+) U87 glioma cells. (A) U87 CD133(+) cells were isolated from the parental U87 cells as described in Materials and Methods Section using MACS technology. Evaluation of CD133 cell surface expression was then performed by flow cytometry on parental U87 and CD133(+) sorted cells. (B) U87 CD133(+) cells were put back into culture and show a typical neurospheres phenotype, unlike their parental counterpart. (C) Total

RNA was extracted from parental U87 and CD133(+) U87 cells and relative gene expression levels assessed by qRT-PCR for CD133 (white bars) and β-actin (black bars). Data are representative of three independent experiments. Probability values of less than 0.05 were considered significant, and an asterisk (*) identifies such significance to the respective parental gene expression.
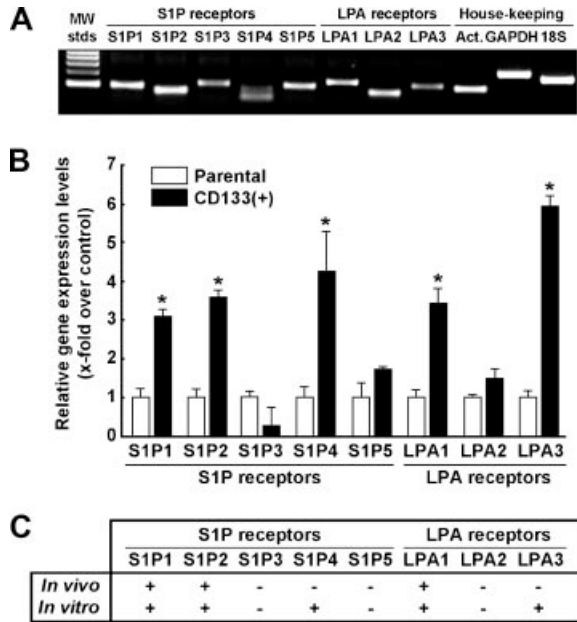
Figure 3. Gene expression levels of the S1P/LPA receptors in CD133(+) U87 glioma cells. Total RNA was extracted from parental (white bars) and CD133(+) (black bars) U87 cells. (A) Validation was performed by semi-quantitative RT-PCR to confirm the presence of a single product amplicon (Act, β-actin; GAPDH, glyceraldehyde 3-phosphate dehydrogenase; 18S, 18S RNA). (B) Relative gene expression levels were then assessed by qRT-PCR for S1P and LPA receptors. Data are expressed as gene expression fold increase in CD133(+) cells relative to parental U87 cells for the individual S1P and LPA receptor genes. Data are representative of three independent experiments. Probability values of less than 0.05 were considered significant, and an asterisk (*) identifies such significance to the respective parental gene expression. (C) Correlation was performed between the in vivo data of Figure 1C and those in vitro data of CD133(+) cells from Figure 3B (+, high expression; −, low expression).

the tumor microenvironment and that could down-regulate the expression of these two genes remains to be further explored.

Migration of CD133(+) U87 Glioma Cells and Erk Phosphorylation Are Increased in Response to the Lysophospholipids Sphingosine 1-Phosphate and Lysophosphatidic Acid

We next assessed the migratory response of CD133(+) cells to S1P and to LPA. While parental U87 glioma cell migration was induced by increasing concentrations of either S1P or LPA (open circles in Figure 4A and B respectively), that of CD133(+) U87 cells was significantly higher than that of the parental cells (closed circles in Figure 4A and B respectively) with optimal migration peaking at ~1 μM lysophospholipid in each case. Interestingly, the LPA-induced increase in cell migration was maintained by concentrations up to 10 μM while the S1P-induced cell migration was maximal at 1 μM for both parental and CD133(+) U87 cells, decreasing dramatically at 10 μM. These observations suggest that, at physiological S1P or LPA concentrations (0.1–1 μM), the response of CD133(+) U87
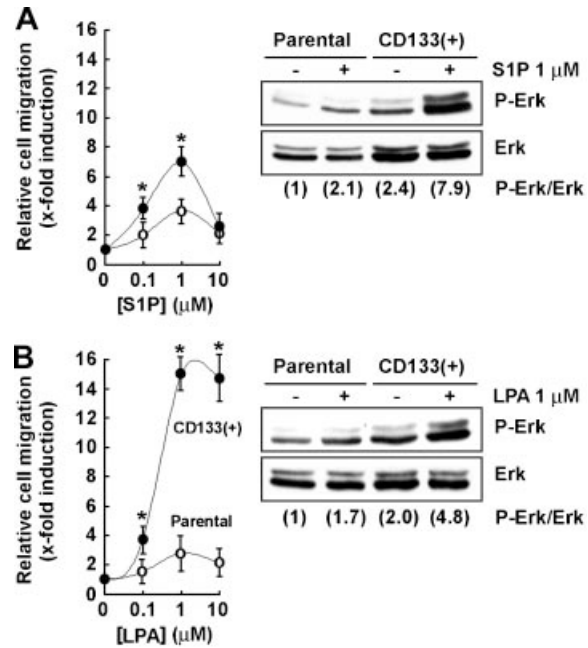

Figure 4. Migration of CD133(+) U87 glioma cells and ERK phosphorylation are increased in response to the lysophospholipids sphingosine 1-phosphate and lysophosphatidic acid. Cell migration (50×10^3 cells/filter, 6 h migration) of parental (white circles) and CD133(+) (black circles) U87 cells was assessed in modified Boyden chambers as described in Materials and Methods Section in the presence of different concentrations of (A) S1P (left panel) or (B) LPA (left panel). Relative cell migration was quantified and expressed as x-fold induction over basal migration (parental U87: 35 ± 6 cells/field; CD133(+) cells: 52 ± 8 cells/field), and values shown represent the means $\pm$ SD of a representative experiment where five random fields per filter were counted for each condition. The extent of ERK phosphorylation was assessed in parental and CD133(+) U87 glioma cell lysates (20 μg protein) isolated from a 1 min incubation with (A) S1P (right panel) or a 2 min incubation with (B) LPA (right panel) and data quantified by scan densitometry and represented as P-Erk/Erk ratios in between brackets (data of one representative experiment out of two).

glioma cells may significantly contribute to the infiltrating phenotype associated with brain tumor development. The extent of S1P- or LPA-mediated intracellular signaling was also assessed in parental and CD133(+) U87 cells by measuring the levels of Erk phosphorylation and expressed as P-Erk/Erk ratios (values in between brackets). We found that lysates isolated from S1P- and LPA-stimulated cells exhibited increased levels of Erk phosphorylation, which response was potentialized in CD133(+) cells in comparison to parental U87 glioma cells (right panels in Figure 4A and B). This increased intracellular signaling capacity, in part, sheds light on the increased migration potential observed in CD133(+) U87 cells.

A Role for MT1-MMP in the Differential Regulation of S1P- and LPA-Mediated Cell Migration and ERK Phosphorylation in Parental and CD133(+) U87 Cells

In order to evaluate the contribution of MT1-MMP towards the increased migratory response to S1P/LPA

in CD133(+) U87 cells, specific gene silencing was used to downregulate MT1-MMP expression, followed by cell migration assays in the presence or absence of S1P or LPA. MT1-MMP knockdown was performed in parental and in CD133(+) cells, and was compared to untransfected (Mock) cells. MT1-MMP gene silencing efficiency was assessed by treating the cells with ConA, a lectin capable of inducing proMMP-2 activation through an MT1-MMP-mediated mechanism. While original CD133 expression was retained in parental and CD133(+) upon siMT1-MMP-transfected cells (not shown), we found that ConA triggered proMMP-2 activation

into MMP-2 in both parental and CD133(+) cells as assessed by gelatin zymography, but that MT1-MMP functions were abrogated in siMT1-MMP-transfected cells (Figure 5A). When cell migration was assessed we found, as expected that both S1P and LPA induced cell migration in parental and CD133(+) cells (Figure 5B, gray bars). On the other hand, neither S1P nor LPA were able to induce cell migration in the parental cells in which MT1-MMP expression was repressed (Figure 5B, parental black bars). Interestingly, while S1P-induced cell migration was also abrogated in siMT1-MMP-transfected CD133(+) cells, LPA-induced cell migration was
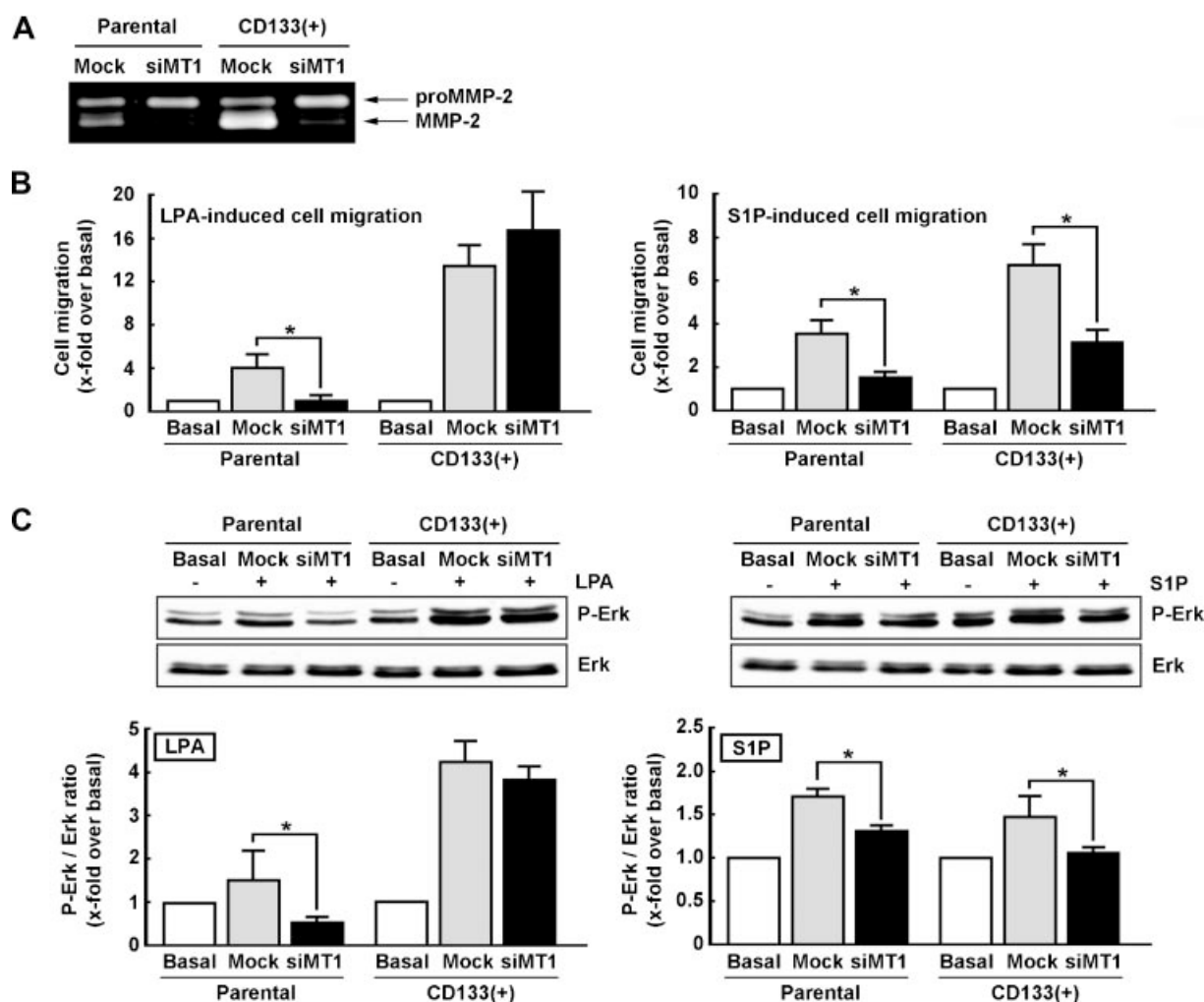

Figure 5. A role for MT1-MMP in the differential regulation of S1P- and LPA-mediated cell migration and ERK phosphorylation in parental and CD133(+) U87 cells. Gene silencing using siRNA was used to downregulate the expression of MT1-MMP in parental and CD133(+) U87 cells as described in Materials and Methods Section. (A) In order to assess MT1-MMP silencing, cells were serum-starved in the presence of Concanavalin-A, a condition shown to trigger proMMP-2 activation through a MT1-MMP-mediated mechanism. Conditioned media from each condition was harvested 48 h post-transfection and the extent of proMMP-2 activation into MMP-2 assessed using gelatin zymography. (B) LPA- and S1P-induced cell migration of parental and CD133(+) U87 cells was assessed as described in Figure 4 in the presence of 1 μM LPA (left panel) or S1P (right panel) in mock (gray bars) and siMT1-MMP-transfected cells (siMT1, black bars). Results are expressed as the x-fold induction over respective basal migration of mock and siMT1-transfected cells (collectively represented by white bars) in parental and CD133(+) cells. (C) A representative Western blot of the extent of Erk phosphorylation was also assessed in those same mock or siMT1-MMP-transfected cells upon 1 μM LPA or S1P stimulation (20 μg protein/well), and data quantified by scan densitometry and represented as P-Erk/Erk ratios from three independent experiments. Probability values of less than 0.05 were considered significant, and an asterisk (*) identifies such significance to the respective Mock value in cell migration and in P-Erk/Erk ratios.

found unaffected (Figure 5B, CD133(+) black bar). These results suggest that an MT1-MMP/S1P intracellular signaling axis is crucial for the increased response to LPA/S1P in glioma cells. Such a signaling axis, however, may be inoperative in the LPA induction of CD133(+) cells resulting in a sustained response to LPA. This was further confirmed by assessing MT1-MMP impact in S1P/LPA-mediated Erk phosphorylation assay in both cell lines. We found that downregulating MT1-MMP expression antagonized S1P-mediated Erk phosphorylation in both parental and CD133(+) U87 cells (Figure 5C), while MT1-MMP lack of expression only affected parental but not CD133(+) cells' response to LPA intracellular signaling leading to Erk phosphorylation (Figure 5C).

DISCUSSION

The CD133(+) stem cell population in brain tumors is highly tumorigenic [26] and shares many of the characteristics of normal tissue stem cells, which might explain clinical features such as tumor metastasis and therapy resistance [27]. CD133(+) cells are also enriched in recurrent gliomas [3], and recent screening of a large panel of glioma samples demonstrated frequencies of CD133(+) cells that increased with tumor grade [6]. The latter study was, in fact, the first to provide strong supporting evidence for the CSC model and for the clinical relevance of the CD133(+) cell population in gliomas. The CSC model has further been described to be locally restricted to a stem cell niche, which size and degree of organization in a particular tumor is believed to be an important factor in determining the clinical course of disease [28]. It is thought that in brain tumors CSC reside in close proximity to blood vessels involved in the irrigation of these vascular niches [7,29]. Whether these vascular niches are preferentially deserved by circulating growth factors is unknown.

Lysophospholipids have been reported to regulate a diverse range of stem cell processes including proliferation, survival, differentiation and migration in adult and embryonic stem cells and progenitors [11]. Whereas lysophospholipids are likely to play a substantial role in mobilization and homing of stem cells, their impact upon the invasive and infiltrative phenotype of brain CSC remains poorly documented. Our study provides evidence that CD133(+) cells are much more responsive to lysophospholipids than are their parental counterparts, partly through differential S1P/LPA receptor expression. In fact, we observed that S1P1, S1P2 and LPA1 appear to be the receptors whose expression is both increased in experimental intracranial tumors and in CD133(+) U87 cells, and which may potentially be responsible for the increased response to S1P and to LPA in CD133(+) U87 cells. Moreover, S1P4 and LPA3 gene expression was also found increased in in vitro-

selected CD133(+) U87 cells, but not in i.c. tumors, suggesting possible in vivo selective pressure of the respective expression of lysophospholipids receptors. The definitive identity of the S1P/LPA receptors involved may be confirmed in the future from specific siRNA approaches. Given that metalloproteinases have been shown to be associated with glioblastoma cell invasiveness [30,31], we further showed that MT1-MMP functions are required in the responsive mechanisms that regulate S1P receptor-mediated signaling. Moreover, in line with the CD133(+) tumor cell phenotype that accounts for glioma stem cell radioresistance [32], expression of MT1-MMP was also increased in several cell line models that escaped radiation-induced apoptosis [33,34]. Previous reports from our laboratory have documented the contribution of MT1-MMP to the infiltrative and invasive phenotype of brain tumor-derived cells [35,36], and impaired MT1-MMP function was also shown to abrogate experimental tumor growth in mice [37]. Strategies which inhibit MT1-MMP activities and/or expression may therefore be envisioned to reduce tumorogenicity and most likely MT1-MMP cooperation to S1P receptor-mediated signaling [36,38].

The recent demonstration that MT1-MMP plays a role in medulloblastoma CD133(+) neurosphere-like formation [18] supports the need to design new therapeutic strategies that either directly target MT1-MMP functions or its associated signaling. Based on blocking its activity with inhibitors, antibodies or RNAi, novel anticancer approaches using inhibition of MT1-MMP activity have already been described [39]. Work with MT1-MMP shows that interference with its RNA expression also decreased tumor cell migration and invasion [40,41]. This approach has been shown to be possible for endothelial cells where interference of MT1-MMP RNA expression decreased the ability to form capillary tubes in the Matrigel system [42]. Although speculative, it is tempting to suggest that therapeutic use of interference RNA approaches could also target the MT1-MMP cooperative functions associated with the S1P response in CD133(+) brain CSC. Evidence provided from the current study suggests that inhibiting MT1-MMP gene expression specifically impairs the response to S1P, but not to LPA, and abrogates CD133(+) glioma cell invasive properties. The future identification of which exact S1P receptor is really responsible for the cell migratory response to S1P via MT1-MMP will further help our comprehension in this unusual cooperative function.

It is still unclear whether CD133 expression plays a causative, contributing or correlative role in formation of the CSC population. Still, among the implications that arise from our study is that the radioresistant phenotype can be ascribed to CD133-expressing CSC [32]. Given that MT1-MMP expression is also correlated with brain tumor recurrence,

increased invasiveness, and radioresistance [33], one can hypothesize that targeting MT1-MMP functions and/or expression may alter the radioresistant and invasive phenotype of brain CSC. The expression of a major group of MT-MMP was recently been found to be elevated in gliomas [43], from which CD133(+) CSC isolated from fresh brain tumor specimens were found to escape the lethal damage of ionizing radiation [32]. New possibilities for abrogating the tumor-promoting function of MT1-MMP, other than the conventional protease inhibitor-based approach, have recently been envisioned [39,44,45].

Alternative molecular therapeutics targeting S1P metabolism and signaling have recently highlighted the antitumor efficacy of FTY720, a sphingosine analogue that can be phosphorylated and that is capable of binding S1P receptors [46] and of sphingomab, an anti-S1P immunoneutralizing monoclonal antibody [47]. Moreover, pharmacological inhibitors such as VPC23019 targeting both S1P1 and S1P3 signaling, JTE013 and VPC44116 respectively targeting S1P2 and S1P1 are available, but to date will not allow one to discriminate for alternate S1P/LPA receptors signaling that could be involved. The emergence of lysophospholipids and their receptors in cancer development suggests implementation of preclinical and clinical evaluation of S1P and LPA as therapeutic targets [9]. In light of these observations, and although it is not yet clear which S1P or LPA receptors are critical targets in CSC, one can confidently speculate that targeting lysophospholipids and their metabolic pathways in CSC may become an attractive therapeutic avenue to explore.

ACKNOWLEDGMENTS

REFERENCES

1. Gagner JP, Law M, Fischer I, Newcomb EW, Zagzag D. Angiogenesis in gliomas: Imaging and experimental therapeutics. Brain Pathol 2005;15:342–363.
2. Gerstner ER, Duda DG, di Tomaso E, Sorensen G, Jain RK, Batchelor TT. Antiangiogenic agents for the treatment of glioblastoma. Expert Opin Investig Drugs 2007;16:1895–1908.
3. Liu G, Yuan X, Zeng Z, et al. Analysis of gene expression and chemoresistance of CD133+ cancer stem cells in glioblastoma. Mol Cancer 2006;5:67.
4. Dell'albani P. Stem cell markers in gliomas. Neurochem Res 2008;33:2407–2415.
5. Wu A, Oh S, Wiesner SM, et al. Persistence of CD133+ cells in human and mouse glioma cell lines: Detailed characterization of GL261 glioma cells with cancer stem cell-like properties. Stem Cells Dev 2008;17:173–184.
6. Zeppernick F, Ahmadi R, Campos B, et al. Stem cell marker CD133 affects clinical outcome in glioma patients. Clin Cancer Res 2008;14:123–129.
7. Gilbertson RJ, Rich JN. Making a tumour's bed: Glioblastoma stem cells and the vascular niche. Nat Rev Cancer 2007;7:733–736.
8. Oka N, Soeda A, Inagaki A, et al. VEGF promotes tumorigenesis and angiogenesis of human glioblastoma stem cells. Biochem Biophys Res Commun 2007;360:553–559.
9. Murph M, Tanaka T, Liu S, Mills GB. Of spiders and crabs: The emergence of lysophospholipids and their metabolic pathways as targets for therapy in cancer. Clin Cancer Res 2006;12:6598–6602.
10. Murph M, Mills GB. Targeting the lipids LPA and S1P and their signalling pathways to inhibit tumour progression. Expert Rev Mol Med 2007;9:1–18.
11. Pébay A, Bonder CS, Pitson SM. Stem cell regulation by lysophospholipids. Prostaglandins Other Lipid Mediat 2007;84:83–97.
12. Young N, Van Brocklyn JR. Roles of sphingosine-1-phosphate (S1P) receptors in malignant behavior of glioma cells. Differential effects of S1P2 on cell migration and invasiveness. Exp Cell Res 2007;313:1615–1627.
13. Anelli V, Gault CR, Cheng AB, Obeid LM. Sphingosine kinase 1 is up-regulated during hypoxia in U87MG glioma cells. Role of hypoxia-inducible factors 1 and 2. J Biol Chem 2008;283:3365–3375.
14. Hemmati HD, Nakano I, Lazareff JA, et al. Cancerous stem cells can arise from pediatric brain tumors. Proc Natl Acad Sci USA 2003;100:15178–15183.
15. Yuan X, Curtin J, Xiong Y, et al. Isolation of cancer stem cells from adult glioblastoma multiforme. Oncogene 2004;23:9392–9400.
16. Blazek ER, Foutch JL, Maki G. Daoy medulloblastoma cells that express CD133 are radioresistant relative to CD133- cells, and the CD133+ sector is enlarged by hypoxia. Int J Radiat Oncol Biol Phys 2007;67:1–5.
17. Dean M, Fojo T, Bates S. Tumour stem cells and drug resistance. Nat Rev Cancer 2005;5:275–284.
18. Annabi B, Rojas-Sutterlin S, Laflamme C, et al. Tumor environment dictates medulloblastoma cancer stem cell expression and invasive phenotype. Mol Cancer Res 2008;6:907–916.
19. Langlois S, Gingras D, Béliveau R. Membrane type 1-matrix metalloproteinase (MT1-MMP) cooperates with sphingosine 1-phosphate to induce endothelial cell migration and morphogenic differentiation. Blood 2004;103:3020–3028.
20. Annabi B, Thibeault S, Lee YT, et al. Matrix metalloproteinase regulation of sphingosine-1-phosphate-induced angiogenic properties of bone marrow stromal cells. Exp Hematol 2003;31:640–649.
21. Meriane M, Duhamel S, Lejeune L, Galipeau J, Annabi B. Cooperation of matrix metalloproteinases with the RhoA/Rho kinase and mitogen-activated protein kinase kinase-1/extracellular signal-regulated kinase signaling pathways is required for the sphingosine-1-phosphate-induced mobilization of marrow-derived stromal cells. Stem Cells 2006;24:2557–2565.
22. Fortier S, Labelle D, Sina A, Moreau R, Annabi B. Silencing of the MT1-MMP/G6PT axis suppresses calcium mobilization by sphingosine-1-phosphate in glioblastoma cells. FEBS Lett 2008;582:799–804.
23. Neth P, Ciccarella M, Egea V, Hoelters J, Jochum M, Ries C. Wnt signaling regulates the invasion capacity of human mesenchymal stem cells. Stem Cells 2006;24:1892–1903.
24. Currie JC, Fortier S, Sina A, Galipeau J, Cao J, Annabi B. MT1-MMP down-regulates the glucose 6-phosphate transporter expression in marrow stromal cells: A molecular link between pro-MMP-2 activation, chemotaxis, and cell survival. J Biol Chem 2007;282:8142–8149.
25. Shmelkov SV, Meeus S, Moussazadeh N, et al. Cytokine preconditioning promotes codifferentiation of human fetal

liver CD133+ stem cells into angiomyogenic tissue. Circulation 2005;111:1175–1183.

26. Singh SK, Hawkins C, Clarke ID, et al. Identification of human brain tumour initiating cells. Nature 2004;432:396–401.

27. Vescovi AL, Galli R, Reynolds BA. Brain tumour stem cells. Nat Rev Cancer 2006;6:425–436.

28. Hope KJ, Jin L, Dick JE. Acute myeloid leukemia originates from a hierarchy of leukemic stem cell classes that differ in self-renewal capacity. Nat Immunol 2004;5:738–743.

29. Calabrese C, Poppleton H, Kocak M, et al. A perivascular niche for brain tumor stem cells. Cancer Cell 2007;11:69–82.

30. Lakka SS, Gondi CS, Rao JS. Proteases and glioma angiogenesis. Brain Pathol 2005;15:327–341.

31. Nakada M, Okada Y, Yamashita J. The role of matrix metalloproteinases in glioma invasion. Front Biosci 2003;8:e261–e269.

32. Bao S, Wu Q, McLendon RE, et al. Glioma stem cells promote radioresistance by preferential activation of the DNA damage response. Nature 2006;444:756–760.

33. Annabi B, Lee YT, Martel C, Pilorget A, Bahary JP, Béliveau R. Radiation induced-tubulogenesis in endothelial cells is antagonized by the antiangiogenic properties of green tea polyphenol (−) epigallocatechin-3-gallate. Cancer Biol Ther 2003;2:642–649.

34. Wild-Bode C, Weller M, Rimner A, Dichgans J, Wick W. Sublethal irradiation promotes migration and invasiveness of glioma cells: Implications for radiotherapy of human glioblastoma. Cancer Res 2001;61:2744–2750.

35. Annabi B, Thibeault S, Moumdjian R, Béliveau R. Hyaluronan cell surface binding is induced by type I collagen and regulated by caveolae in glioma cells. J Biol Chem 2004;279:21888–21896.

36. Annabi B, Bouzeghrane M, Moumdjian R, Moghrabi A, Béliveau R. Probing the infiltrating character of brain tumors: Inhibition of RhoA/ROK-mediated CD44 cell surface shedding from glioma cells by the green tea catechin EGCg. J Neurochem 2005;94:906–916.

37. Nyalendo C, Beaulieu E, Sartelet H, et al. Impaired tyrosine phosphorylation of membrane type 1-matrix metalloproteinase reduces tumor cell proliferation in three-dimensional matrices and abrogates tumor growth in mice. Carcinogenesis 2008;29:1655–1664.

38. Annabi B, Lachambre MP, Bousquet-Gagnon N, Page M, Gingras D, Beliveau R. Green tea polyphenol (−)-epigallocatechin 3-gallate inhibits MMP-2 secretion and MT1-MMP-driven migration in glioblastoma cells. Biochim Biophys Acta 2002;1542:209–220.

39. Arroyo AG, Genís L, Gonzalo P, Matías-Román S, Pollán A, Gálvez BG. Matrix metalloproteinases: New routes to the use of MT1-MMP as a therapeutic target in angiogenesis-related disease. Curr Pharm Des 2007;13:1787–1802.

40. Bartolomé RA, Molina-Ortiz I, Samaniego R, Sánchez-Mateos P, Bustelo XR, Teixidó J. Activation of Vav/Rho GTPase signaling by CXCL12 controls membrane-type matrix metalloproteinase-dependent melanoma cell invasion. Cancer Res 2006;66:248–258.

41. Ueda J, Kajita M, Suenaga N, Fujii K, Seiki M. Sequence-specific silencing of MT1-MMP expression suppresses tumor cell migration and invasion: Importance of MT1-MMP as a therapeutic target for invasive tumors. Oncogene 2003;22:8716–8722.

42. Robinet A, Fahem A, Cauchard JH, et al. Elastin-derived peptides enhance angiogenesis by promoting endothelial cell migration and tubulogenesis through upregulation of MT1-MMP. J Cell Sci 2005;118:343–356.

43. Nuttall RK, Pennington CJ, Taplin J, et al. Elevated membrane-type matrix metalloproteinases in gliomas revealed by profiling proteases and inhibitors in human cancer cells. Mol Cancer Res 2003;1:333–345.

44. Hatakeyama H, Akita H, Ishida E, et al. Tumor targeting of doxorubicin by anti-MT1-MMP antibody-modified PEG liposomes. Int J Pharm 2007;342:194–200.

45. Nonaka T, Nishibashi K, Itoh Y, Yana I, Seiki M. Competitive disruption of the tumor-promoting function of membrane type 1 matrix metalloproteinase/matrix metalloproteinase-14 in vivo. Mol Cancer Ther 2005;4:1157–1166.

46. Brinkmann V, Cyster JG, Hla T. FTY720: Sphingosine 1-phosphate receptor-1 in the control of lymphocyte egress and endothelial barrier function. Am J Transplant 2004;4:1019–1025.

47. Visentin B, Vekich JA, Sibbald BJ, et al. Validation of an anti-sphingosine-1-phosphate antibody as a potential therapeutic in reducing growth, invasion, and angiogenesis in multiple tumor lineages. Cancer Cell 2006;9:225–238.